UNIVERSITY OF OKLAHOMA

GRADUATE COLLEGE

ANHYDRITE NUCLEATION AND GROWTH AT LOW TEMPERATURES: EFFECTS OF FLOW RATE, ACTIVITY OF WATER, AND MINERAL SUBSTRATES

A THESIS

SUBMITTED TO THE GRADUATE FACULTY

in partial fulfillment of the requirements for the

Degree of

MASTER OF SCIENCE

By

KAYLA MARIE MILLER
Norman, Oklahoma
2017

Downloaded from SHAREOK. Persistent Handle URL: https://hdl.handle.net/11244/50862

ANHYDRITE NUCLEATION AND GROWTH AT LOW TEMPERATURES: EFFECTS OF FLOW RATE, ACTIVITY OF WATER, AND MINERAL SUBSTRATES

A THESIS APPROVED FOR THE
CONOCOPHILLIPS SCHOOL OF GEOLOGY AND GEOPHYSICS

BY

_____
Dr. Megan Elwood Madden, Chair

_____
Dr. Andrew Elwood Madden

_____
Dr. Michael Soreghan

© Copyright by KAYLA MARIE MILLER 2017
All Rights Reserved.

For my family who have long indulged and supported my curiosity about the world

Acknowledgements

I want to acknowledge and thank my committee members Dr. Megan Elwood Madden, Dr. Andrew Elwood Madden, and Dr. Michael Soreghan for being so caring and generous with their time, advice, extraordinarily prompt feedback, and encouragement over the past two years.

I would also like to thank my professors here at OU for sharing their passions for teaching and geology; my collaborators Dr. Charity Phillips-Lander for her help and encouragement in both the lab and the field and Dr. Janice Bishop for her assistance on this project; Greg Strout, Dr. Scott Russell, and Dr. Preston Larson in OU Microscopy for training me on transmission electron microscopes; Dr. Mourad Benamara at the Arkansas Institute for Nanoscale Materials Science for his work with us on high resolution imaging and analyses on a transmission electron microscope; and the OU School of Geology and Geophysics and NASA grant NNX13AG75G for funding this research.

Finally, I want to thank the great friends I've made here in Norman for their openness, acceptance, and heartening support throughout this journey.

Table of Contents

Acknowledgements iv

List of Tables vi

List of Figures vii

Abstract viii

Introduction 1

Observations and previous interpretations of sulfates on Mars 2

Brines on Mars 4

Recent advances in calcium sulfate nucleation and growth 4

Methods 7

Results 12

Jarosite Experiments 12

Carbonate experiments 24

Discussion 29

Results Summary 29

Implications of gypsum formation in jarosite + brine experiments 30

Implications of anhydrite formation in jarosite + brine experiments 31

Implications of possible bassanite formation in jarosite + brine experiments 32

Implications of akaganeite formation in jarosite + brine experiments 33

Carbonate experiment results 36

Implications for Mars 36

Conclusions 39

References 40

List of Tables

Table 1. Jarosite + $CaCl_2$ brine XRD Results..... 13

List of Figures

Figure 1. Experimental setup. 11

Figure 2. XRD results for 22-day flow-through experimental runs - jarosite + brine 14

Figure 3. XRD results for 22-day batch experiment runs - jarosite + brine. 15

Figure 4. Raman spectra of jarosite + brine flow-through experiments. 17

Figure 5. VNIR spectra of 22-day jarosite + brine experiments 19

Figure 6. TEM images (a) batch reactor (large lath shaped crystals) and (b) flow-through experiments (nanoscale mineral nucleation on jarosite surface) suggests variability in nucleation processes. 21

Figure 7. Mineral phases observed in TEM. 22

Figure 8. EDS jarosite alteration in jarosite + flowing brine experiment (left) and corresponding high angle annular dark field STEM images (right). 23

Figure 9. XRD results for 22-day flow-through experiment runs - calcite + brine. 25

Figure 10. XRD results for 22-day batch experiment using calcite + brine. 26

Figure 11. SEM image and EDS maps showing calcite coated with brine residues. 28

Figure 12. Model of suggested heterogeneous calcium sulfate and akageneite nucleation and growth and jarosite in flow-through experiments. 35

Abstract

Understanding calcium sulfate mineral formation is crucial to understanding depositional environments and diagenetic conditions on and near the martian surface where calcium sulfates with varying hydration states have been well documented (e.g. Nachon et al., 2014; Vaniman et al., 2014). Calcium sulfate minerals – anhydrite ($CaSO_4$), bassanite ($CaSO_4 \cdot 0.5H_2O$), and gypsum ($CaSO_4 \cdot 2H_2O$) – are of particular interest because they serve as good indicators of past aqueous environments on Mars.

Traditionally, gypsum was traditionally thought to form at low temperature, independent of salinity due to kinetic effects, while anhydrite is traditionally understood to form at higher temperatures (>50°C), even though anhydrite is more thermodynamically stable at low temperatures in high salinity, low water activity brines. Closed-system batch experiments conducted by various workers (e.g. Posnjak, 1940; Freyer and Voigt, 2003; Ossario et al., 2014) over the last century have confirmed these assumptions. However, recent flow-through experiments conducted by Dixon et al. (2015) demonstrated low temperature anhydrite formation in high salinity brines in flowing hydrodynamic systems over a three-week period while gypsum formed in closed system batch reactor experiments under identical conditions. They hypothesized that anhydrite may form at low temperatures in flow-through experiments due to the constant source of high salinity, low-water activity brine, while gypsum initially nucleates in the batch reactors, increasing the activity of water as calcium and sulfate ions are consumed. Other workers have suggested that anhydrite, bassanite, and gypsum form via complex nucleation, aggregation, and growth processes (e.g. Van Driessche et al., 2012; Stawski et al., 2016). These pre-cursor nucleation and

aggregation phases may be affected by hydrologic flow rates (Dixon et al., 2015), as well as different mineral substrates present in the system (Bystriansky et al., 2016). In this study, we aim to further investigate the role of hydrologic conditions on anhydrite formation at low temperature in flowing brine by testing Dixon et al.'s hypothesis. We also test the effects of varying mineral substrates on calcium sulfate formation by conducting similar experiments reacting calcite ($CaCO_3$) + $MgSO_4$ and $MgCl_2$ brines. We analyzed the reaction products with powder X-ray diffraction, Raman spectroscopy, visible/near infrared spectroscopy, transmission electron microscopy, and scanning electron microscopy.

Our jarosite + brine experimental results confirmed that different calcium sulfate minerals form in flow-through experiments compared to batch experiments, despite identical solution chemistries, reaction time, and temperature conditions. Over a range of $CaCl_2$ concentrations and water activities, anhydrite is only observed in flow-through experiments, while gypsum is observed in both batch and flow-through experiments. Akaganeite is also formed in abundance in all flow-through and batch experiments. Preliminary TEM data show calcium enrichment associated with nanoscale minerals on the edges of jarosite in flow-through experiments. Gypsum was the only calcium sulfate phase identified in batch reactor experiments, where it formed relatively large (>1μm) lath-shaped gypsum crystals in the batch experiments that were not observed in flow-through experiments. These differing mineral assemblages and textures observed in flow-through compared with batch experiments confirm that hydrologic conditions are primary variables affecting calcium sulfate mineralization. No anhydrite was formed in flow-through experiments reacting calcite + sulfate-rich brine, further suggesting

anhydrite formation in jarosite + brine flow-through experiments is controlled by mineral substrate or by the presence of other ions in solution in addition to hydrodynamic conditions.

Previous studies have interpreted anhydrite veins on Mars as forming at depth from pre-existing gypsum indicating significant burial had occurred prior to diagenesis (Vaniman et al., 2014; Bristow et al., 2015). However, our experimental results demonstrate that anhydrite can also form at low temperature from jarosite alteration in $CaCl_2$ brines without a pre-existing gypsum phase if there is groundwater flow. Akaganeite is also observed deposits on Mars. Ultimately, our findings can provide much needed data for interpreting the timing and evolution of depositional environments and diagenetic conditions for the sedimentary rocks at Gale Crater and other locations where calcium sulfate minerals have been observed (e.g. Grotzinger et al., 2015; Stack et al., 2016).

Introduction

Traditionally, gypsum ($CaSO_4 \cdot 2H_2O$) is thought to form at low temperature, independent of salinity due to kinetic effects, whereas anhydrite ($CaSO_4$) only forms at higher temperatures (>50°C), even though anhydrite is more thermodynamically stable at low temperatures in high salinity, low water activity brines. Closed-system batch experiments conducted by various workers (Posnjak, 1940; Zen, 1965; Hardie, 1967; Freyer and Voigt, 2003; Ossario et al., 2014) over the last century have confirmed these assumptions. However, recent flow-through experiments conducted by Dixon et al. (2015) demonstrated low temperature anhydrite formation in high salinity brines in flowing hydrodynamic systems over a three-week period.

This departure from long held assumptions spurred our current work to understand *why* anhydrite readily forms in flow-through reactors while gypsum is the only calcium sulfate phase observed in batch reactors with identical solutions. This query is important because calcium sulfate minerals with varying hydration states, anhydrite ($CaSO_4$), bassanite ($CaSO_4 \cdot 0.5H_2O$), and gypsum ($CaSO_4 \cdot 2H_2O$), are commonly used to interpret the depositional and diagenetic conditions experienced by rocks both on Mars and on Earth. Anhydrite would typically be interpreted to reflect at temperatures exceeding 50° C in high salinity waters, while gypsum is interpreted to reflect lower temperatures across a wide range of water activities (e.g. He et al., 1994; Warren et al., 1989).

Observations and previous interpretations of sulfates on Mars

Sulfate minerals are prevalent on Mars and have been identified via orbiters (Bibring et al., 2006; Langevin et al., 2005), rovers (Squyers et al., 2004; Vaniman et al., 2014), and within martian meteorites (Bridges et al., 2001; McCubbin et al., 2009; Gooding et al., 1988; Gooding et al., 1991). These sulfate mineral assemblages have been used to aid in determining diagenetic conditions experienced on Mars. Jarosite ($KFe^{3+}_3(OH)_6(SO_4)_2$) is widely distributed on Mars and is also observed on Earth in wet acid-sulfate systems, indicating past acidic, oxidizing waters on Mars (Glotch and Rogers, 2007; Elwood Madden et al., 2004). Magnesium sulfates with a range of hydration states are also common phases observed on Mars (e.g. Vaniman et al., 2004; Gendrin et al., 2005). Hydrated sulfate minerals detected on Mars are particularly important because they can be used as an indication of past or ongoing aqueous activity on the martian surface (Gendrin et al., 2005) and as a starting point for workers assessing Mars' habitability (Aubrey et al., 2006; Tosca et al., 2008; Clark, 1978).

Calcium sulfate minerals on Earth can be found in arid, salt-rich depositional environments and are also commonly observed in mineralized fractures as secondary diagenetic phases. On Mars, calcium sulfates are particularly compelling as indicators of past aqueous activity. The three primary calcium sulfate phases – anhydrite, bassanite, and gypsum – have been identified on Mars in sediments deposited within Gale crater where the sulfates are found dispersed in the sediment matrix and as the dominant mineral in complex vein systems (Nachon et al., 2014; Vaniman et al., 2014). Workers have suggested models of bassanite and anhydrite formation on Mars that require relatively high temperatures via hydrothermal fluids (Vaniman et al., 2008) or

significant burial (Bristow et al., 2015) to dehydrate gypsum to form bassanite and anhydrite (Vaniman et al., 2017). However, low temperature conditions are more relevant to near surface processes on Mars. Analyses of sediments at Yellowknife Bay, Gale Crater indicate temperatures less than 70°C (Vaniman et al., 2014; Grotzinger et al., 2014, Bristow et al., 2015; Borlina et al., 2015) and minimal burial diagenetic alteration (Bristow et al., 2016). Therefore, Vaniman et al. (2017) suggested that the co-occurrence of gypsum, anhydrite, and bassanite in martian sedimentary strata is a product of gypsum dehydration as the sediments are re-exhumed at the surface during extended exposure over many summers rather than as a result of discrete diagenetic events.

Previous experiments have shown that anhydrite and gypsum can also form at low temperature through jarosite reacting with $CaCl_2$ brines. Dixon et al. (2015) performed flow-through experiments at 22°C reacting jarosite + 50 wt. % $CaCl_2$ brine and found anhydrite precipitating in high salinity brines over 3 weeks while gypsum formed in otherwise identical batch reactors. They hypothesized that anhydrite may form at low temperatures in flow-through experiments due to the constant source of high salinity, low-water activity brine, while gypsum initially nucleates in the batch reactors, increasing the activity of water as calcium and sulfate ions are consumed. Other workers have suggested that anhydrite, bassanite, and gypsum form via complex nucleation, aggregation, and growth processes (Van Driessche et al., 2012; Ossario et al., 2014; Stawski et al., 2016). These pre-cursor nucleation and aggregation phases may be affected by hydrologic flow rates (Dixon et al., 2015), as well as different mineral substrates present in the system (Bystriansky et al., 2016).

Brines on Mars

Jarosite + brine experiments are relevant to Mars because brines represent the only stable liquid water possible near the martian surface over much of Mars' recent history due to low surface temperatures and pressures. The primary evidence for the presence of brines on Mars comes from the detection of high chlorine and sulfate abundances (Brass, 1980), orbiter and rover detected hydrated mineral phases (Langevin et al., 2005; Mangold et al., 2008), and the observation of recurring slope lineae (Ojha et al., 2014). Salts and chloride minerals that have been detected in situ in martian soils and dust (e.g. Clark, 1993; Rieder et al., 2004; Yen et al., 2005; Wang et al., 2006; Hecht et al., 2009) as well as spectra of rocks and soils collected by Mars rovers (e.g. Christensen et al., 2004; Klingelhöfer et al., 2004; McLennan et al., 2005; Arvidson et al., 2006; Hecht et al., 2009; Rao et al., 2009; Hurowitz and Fischer, 2014; Toner et al., 2014) and from satellite data (e.g. Glotch and Christensen, 2005; Langevin et al., 2005; Bibring et al., 2006; Osterloo et al., 2008; Ehlmann et al., 2008; Murchie et al., 2009; Weitz et al., 2015). Understanding both the composition and behavior of martian brines is central to larger questions about Mars' hydrologic cycle and the possibility of past or current habitable conditions at or near the martian surface. Here, we investigate the formation of calcium sulfates via brine + mineral interactions to further understand the role(s) brines may have played in near surface processes.

Recent advances in calcium sulfate nucleation and growth

Calcium sulfate nucleation and growth at low temperatures have been studied in many contexts including foundational mineralogy (Pina, 2009), scale precipitation in

industrial applications (Bystriansky et al., 2016), materials synthesis (Wang et al., 2012) and planetary geology (Dixon et al., 2015). Notable studies include Sohnel and Garside (1992) and Mullin (1993) who found that homogeneous nucleation should drive calcium sulfate mineral formation in supersaturated solutions with no dispersed particles but that heterogeneous nucleation prevails when foreign particles or surfaces are present in the system. They found that regions of metastability and the induction time required for calcium sulfate formation were significantly reduced when particles were present in the system. Bystriansky et al. (2016) also found that the presence of iron (Fe^{3+}) in the solution reduced induction time and accelerated crystallization and that reverse osmosis (flow-through) systems require shorter crystallization time than jar (batch) experiments under otherwise identical conditions.

Pina (2009) studied anhydrite dissolution and growth at low (room) temperature in pure water and found that both anhydrite dissolution and growth were crystallographically controlled. In this study, anhydrite grew as monolayer expansions on the previous anhydrite surface, despite anhydrite's metastability in the system relative to gypsum (Pina, 2009). Wang et al. (2012) showed that in homogeneous systems (no particles present to serve as nucleation sites) amorphous calcium sulfate and bassanite are precipitated prior to gypsum, then aggregate to form gypsum in bulk, documenting the first experimental observation of amorphous calcium sulfate and bassanite forming at low temperature, low salinity conditions prior to gypsum. Interestingly, the paper also notes a biological example of bassanite formation under ambient, low salt conditions "courtesy of the humble jellyfish" where bassanite and gypsum have been identified as the gravity sensors of deep-sea medusae. While these

calcium sulfates are obviously biominerals, they show a significant pathway for the formation of bassanite and gypsum from solution in ambient conditions.

Calcium sulfate nucleation and growth is governed by complex interplay between thermodynamics, kinetics, and – as we suggest here – mineralogy and hydrodynamic conditions. Recent work suggests that reevaluating long-held assumptions about low temperature calcium sulfate formation and embracing a more complicated system that considers heterogeneous nucleation pathways, mineralogy, and hydrodynamic conditions can yield more realistic interpretations of near surface processes both on Mars and on Earth.

Here, we aim to further investigate the role of hydrologic conditions on anhydrite formation at low temperature in flowing brine by testing Dixon et al.'s hypothesis that anhydrite may form at low temperatures in flow-through experiments due to the constant source of high salinity, low water-activity brine, while gypsum initially nucleates in the batch reactors, increasing the activity of water as calcium and sulfate ions are consumed by varying brine concentration under identical conditions in flowing and batch (closed) system experiments. We also testthe effects of varying mineral substrates on calcium sulfate formation by conducting similar experiments reacting calcite ($CaCO_3$) + $MgSO_4$ and $MgCl_2$ brines.

Methods

We conducted flow-through and batch experiments reacting jarosite with $CaCl_2$ brine of varying water activities at room conditions based on established methods (Dixon et al. 2015). Then, we conducted a second set of flow-through and batch experiments reacting calcite with $MgSO_4$+$MgCl_2$ brine of varying water activities under the same conditions to compare the effects of different mineral substrates/reactant sources on calcium sulfate formation and mineralogy. We determined mineral phases present in experimental samples using powder X-ray diffraction, Raman spectroscopy, visible/near infrared spectroscopy, and transmission electron microscopy for jarosite + brine experiments. For calcite + brine experiments, we used powder X-ray diffraction and scanning electron microscopy to characterize the reaction products.

We used the same batch of K-jarosite ($K_{0.99}Fe_{2.93}(SO_4)_{2.04}(OH)_6$) that was synthesized and studied by Dixon et al. (2015) using the method developed by Driscoll and Leinze (2005). The material was previously characterized using powder x-ray diffraction and electron probe microanalysis (Dixon et al. 2015). We conducted flow-through experiments with synthetic K-jarosite + 5 wt. % ($a_w = 0.98$), 20 wt. % ($a_w = 0.8$), and 50 wt. % ($a_w = 0.5$) $CaCl_2$ brine at room temperature and pressure over 10 days to test the effects of brine concentration on mineral reaction products. Identical 22-day experiments were also conducted using 5 wt. % and 20 wt. % $CaCl_2$ brines, and 22-day 50 wt. % experimental data was taken from Dixon et al. (2015). We also conducted closed system batch reactor experiments under otherwise identical conditions to compare mineralogy with flow-through experiments by combining 150 mL of $CaCl_2$ brine with

0.5 g of synthetic K-jarosite. We used volumetric flasks covered with parafilm and let the closed-system experiments react on an oscillating shaker table for 10 days, sampled them, and then returned the reactors to the shaker table until the experiment reached 22 days. We vacuum filtered the brine + mineral slurry samples prior to analysis.

Similar flow-through and batch reactor experiments were conducted under identical conditions using 5 wt. % and 24 wt. % $MgSO_4$+$MgCl_2$ brine mixtures (1:1 by weight) reacted with optical-grade calcite ($CaCO_3$) as the mineral substrate.

We employed powder X-ray diffraction (XRD) to identify the mineral phases present in both flow-through and batch reactor experiments. We analyzed all samples on zero-background holders with Bragg-Brentano geometry at the University of Oklahoma using a Rigaku Ultima IV diffractometer with a Cu tube operated at 40 kV and 44 mA and a curved graphite monochromator that passes predominantly Cu Kα radiation. All samples were initially analyzed at 4 seconds/step, and 22 day 5 wt. % and 20 wt. % samples were reanalyzed at 16 seconds/step to improve peak intensities.

Due to the relative insensitivity of XRD to poorly crystalline or nanocrystalline phases within the jarosite matrix, we used Raman spectroscopy as a secondary analytical technique to identify and map mineral phases present in the samples, employing a Renishaw inVia confocal Raman microscope with 785nm laser at 1% power with 1200 lines/cm grating located at the University of Oklahoma. We conducted spot analyses over a spectral range of 49-1273 cm^{-1} with a center position at 700 cm^{-1}. The data presented here was baseline corrected and normalized using WiRE software.

We also conducted visible/near-infrared spectroscopy at the SETI Institute to test the possibility of detecting and resolving calcium sulfate phases in these samples.

VNIR spectra were measured at the SETI Institute using a FieldSpecProFR device with a contact probe and solar simulated light source. Reflectance were measured between 0.35-2.5 μm. Several spectra were collected of each jarosite + brine sample, and the spectra were averaged. Collected spectra were compared with spectra of minerals in a library maintained by Janice Bishop.

Finally, we examined the textural relationships in the reaction products using transmission electron microscopy (TEM) to evaluate possible nucleation pathways leading to anhydrite precipitation in flowing brines. We ultrasonicated experimental samples with isopropyl alcohol for 10 minutes before pipetting 7ml of the solution onto lacy carbon formvar TEM grids. We then analyzed the experimental samples using 80kV Zeiss10 (OU), a 200kV JEOL 2000FX (OU), and a 300kV FEI Titan (University of Arkansas) TEMs.

Calcite + brine experiments were analyzed via XRD and scanning electron microscopy (SEM) to identify mineral phases and mineral phase relationships in the experimental samples. We used an FEI Quanta 250 Scanning Electron Microscope with a Bruker Quantax EDS for mapping.

We analyzed XRD data using Jade software and direct peak comparisons between experimental samples. Data analysis was completed using Jade 2010 software with the International Centre for Diffraction Data PDF4+ database. Raman peak positions were mapped with inVia WiRE software. Raman peak comparisons were made against data available in the RRUFF database (Lafuente et al., 2015) for jarosite and calcium sulfate phases; however, akaganeite peak data were compared with data reported in Ohtsuka (1996). We used Kaleidoscope and Excel to graph VNIR data and analyze band positions

against standards previously collected at the SETI Institute. We collected images, EDS data, and diffraction patterns via TEM and analyzed these using Digital Micrograph, Adobe Photoshop, and ImageJ.

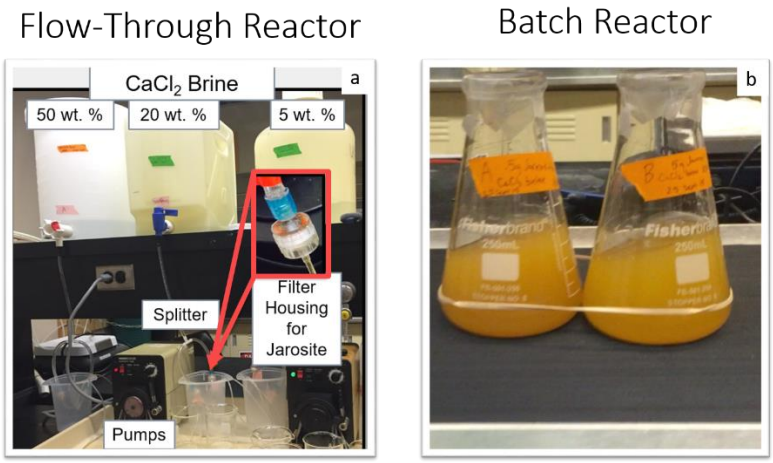

Figure 1. Experimental setup: a) flow-through experimental setup b) batch reactor experimental setup on oscillating shaker table.

Results

Jarosite Experiments

XRD: Akaganeite (FeO(OH,Cl)) is observed as a reaction product across all experiments (Table 1). Antarcticite ($CaCl_2 \cdot 6H_2O$) is also observed in most experiments, but is considered to be present in reaction product specimens due to precipitation of residual brine in the samples and was likely not present in the dissolution reactors. Gypsum is present across all flow-through and batch experiments. Bassanite may be present in trace amounts (less than 1 weight percent) in two flow-through experiments, but is not observed in any of the batch experiments. We observed anhydrite in all of the flow-through experiments but anhydrite was not present in any of the batch experiments.

Table 1. Jarosite + $CaCl_2$ brine XRD Results – phases with "?" indicate trace amounts (<1 wt. %). 22-day 50 wt. % experimental data from Dixon et al. (2015).

EXPERIMENT	50 wt. %	20 wt. %	5 wt. %
a_{H_2O}	0.56	0.88	0.98
BATCH			
10-day	Gypsum Akaganeite	Gypsum Akaganeite	N/A
22-day	Gypsum Akaganeite	Gypsum Akaganeite	N/A
FLOW			
10-day	Anhydrite Gypsum Akaganeite	Anhydrite? Gypsum Akaganeite Bassanite?	Anhydrite Gypsum Akaganeite
22-day	Anhydrite Gypsum Akaganeite	Anhydrite Gypsum Akaganeite	Anhydrite Gypsum Akaganeite Bassanite?

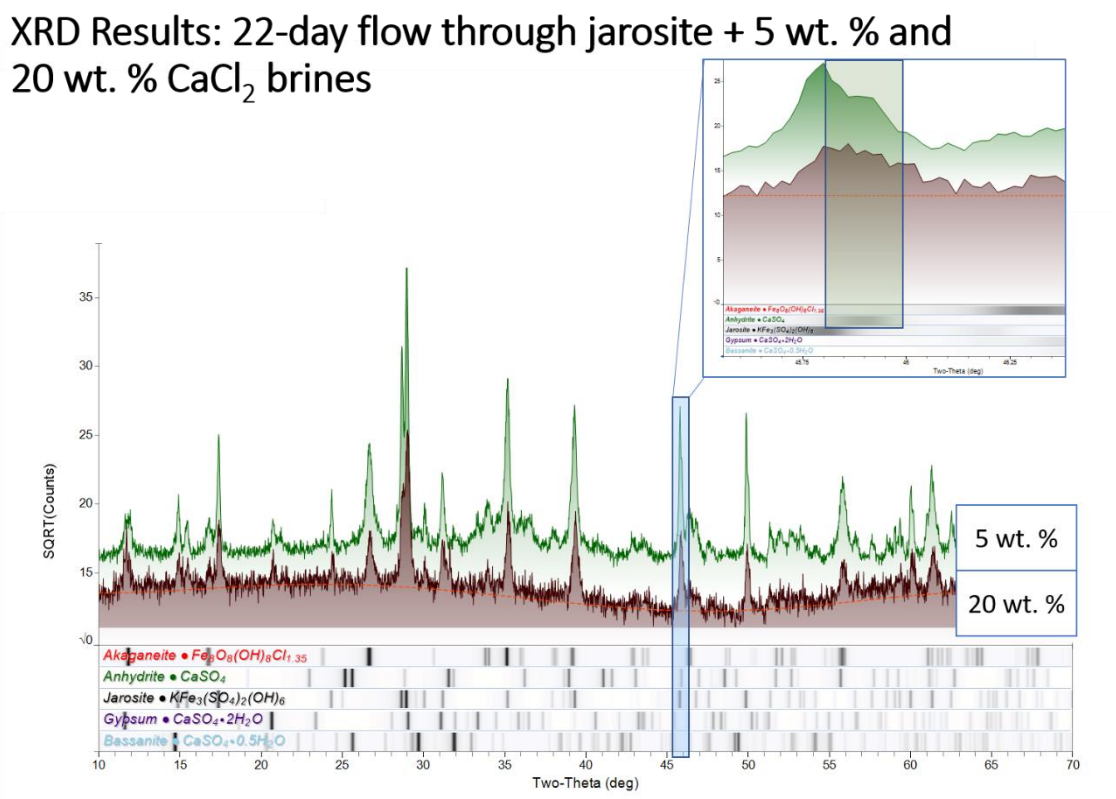

Figure 2. XRD results for 22-day flow-through experimental runs using jarosite + 5 wt. % (green) and 20 wt. % (brown) brines. 16 second/step analyses. Peak positions for akaganeite, anhydrite, jarosite, gypsum, and bassanite are shown below patterns. Magnified area shows detail of anhydrite peak adjacent to jarosite peak at ~ 46º 2θ.

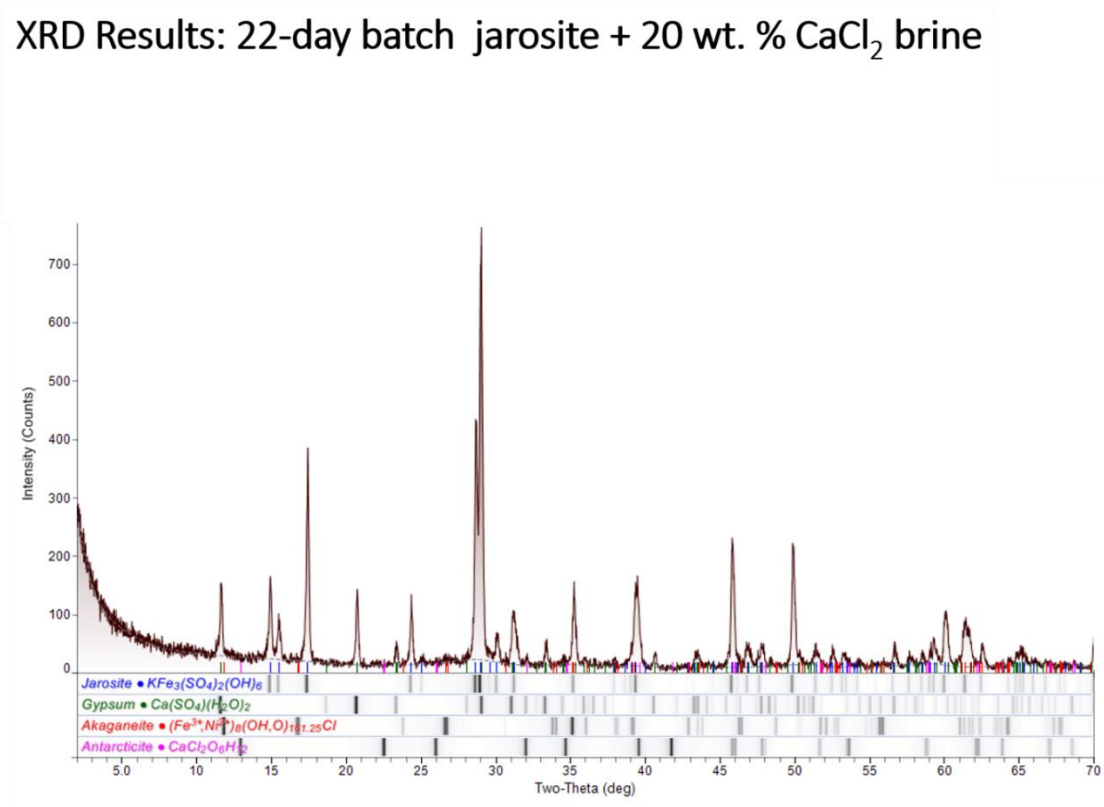

Figure 3. XRD results for 22-day batch experiment runs using jarosite 20 wt. % brines. Peak positions for jarosite, gypsum, akageneite, and antarcticite are shown below patterns.

Raman: Raman spectra collected from experimental samples and jarosite starting material were collected and compared with anhydrite and gypsum spectra from the RRUFF database (Lafuente et al., 2015) and an akaganeite spectrum from Ohtsuka (1996). A broad akaganeite peak is observed between 700-750 cm^{-1}. Similarities in peak shape between the anhydrite and 5 wt. % brine sample are observed in shoulder features at 1029.8 cm^{-1} and 1049.8 cm^{-1}. An anhydrite peak is also observed in the 20 wt. % brine sample at 1136 cm^{-1}. Gypsum peak positions overlap jarosite, anhydrite, or akaganeite positions, but this phase has been well documented in XRD.

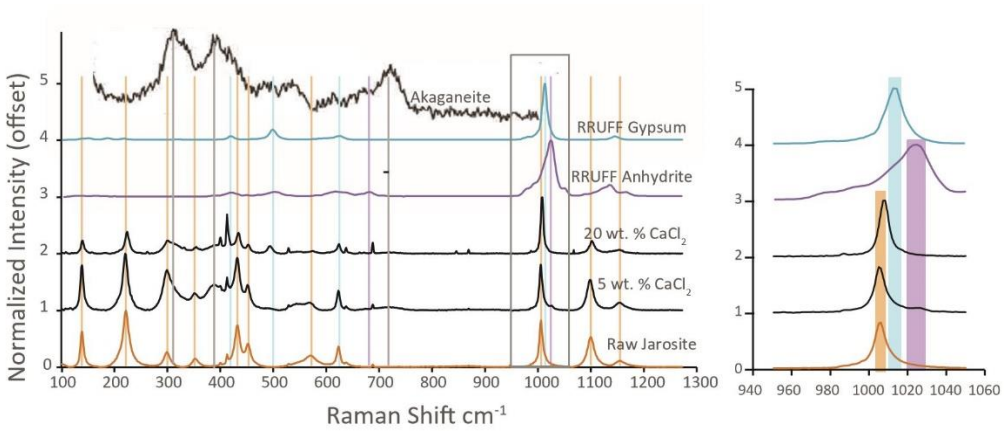

Figure 4. Raman spectra (785 nm laser) of jarosite + 5 wt. % and 20 wt. % $CaCl_2$ brine flow-through experiments. Spectra of unreacted jarosite (orange), anhydrite (purple) and gypsum (blue) from RRUFF database (Lafuente et al., 2015), and akageneite (black, modified from Ohtsuka, 1996) are shown for comparison. Major peaks for each of the reference phases have been highlighted with the vertical bars.

VNIR: VNIR spectra of the samples are dominated by jarosite bands with some possible gypsum features (Figure 5). Anhydrite does not have features in this spectral region. Because no secondary phases were definitively identified in the VNIR spectra, these analyses are not considered further here.

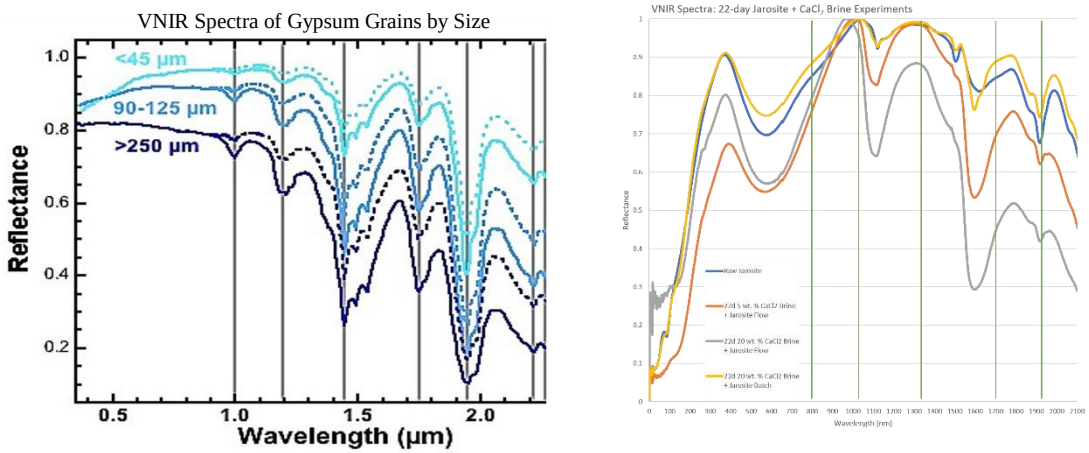

Figure 5. VNIR spectra of gypsum grains by size (left) modified from Bishop et al. (2016) and VNIR spectra of jarosite starting material and 22-day jarosite + $CaCl_2$ brine experiments (right). Green vertical lines indicate gypsum band locations from Bishop et al. (2016).

TEM: Gypsum is the only calcium sulfate phase identified in batch reactor experiments, forming as relatively large (>1μm) lath-shaped crystals observed in TEM analyses (Figure 6a). Though XRD and Raman analyses suggest gypsum and anhydrite are both present in flow-through experiments, the large lath-shaped gypsum particles were not observed in any of the flow-through experiments. Akaganeite is observed around jarosite grains (Figure 6b) and as matted aggregates (Figure 7a) in both batch and flow-through experiments.

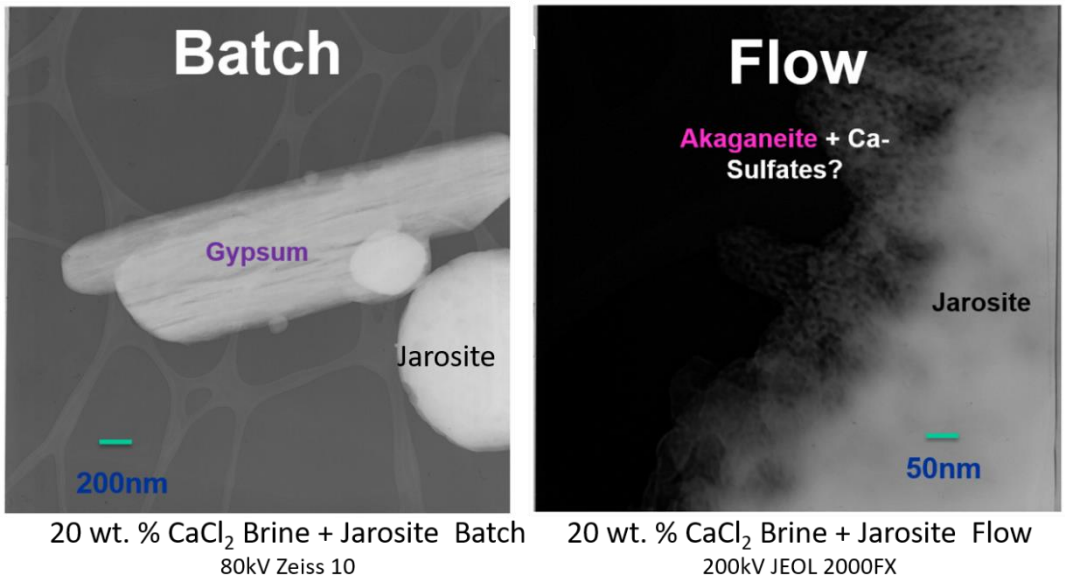

Figure 6. Significant differences between the morphology of calcium sulfate phases between (a) batch reactor (large lath shaped crystals) and (b) flow-through experiments (nanoscale mineral nucleation on jarosite surface) suggests variability in nucleation processes.

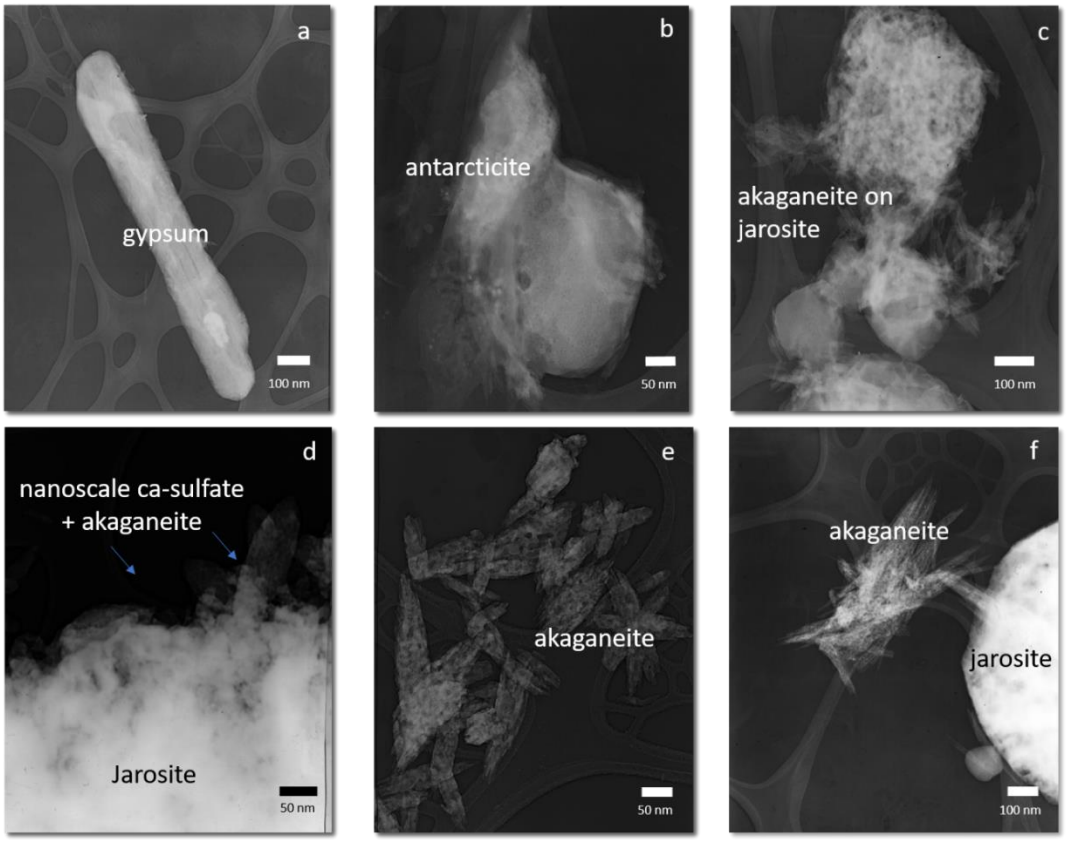

Figure 7. Mineral phases observed in TEM. (a-c) 22-day 20 wt. % $CaCl_2$ brine + jarosite batch experiments. (d-f) 22-day 20 wt. % $CaCl_2$ brine + jarosite flow-through experiments. All images acquired on 200kV JEOL 2000 FX.

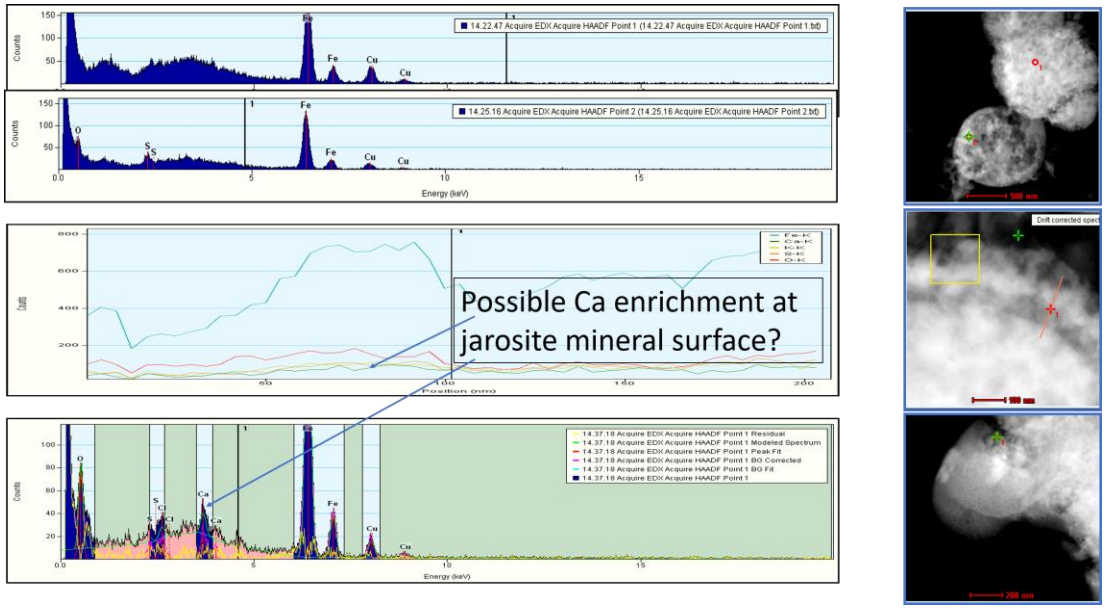

Figure 8. Energy dispersive X-ray spectroscopy of jarosite alteration in jarosite + 20 wt.% $CaCl_2$ flowing brine experiment (left) and corresponding high angle annular dark field STEM images (right).

Carbonate experiments

XRD: In the 5 wt. % $MgSO_4$ + $MgCl_2$ brine flow-through experiments, calcite is the dominant phase observed with secondary phases either absent or below detection limits (Figure 10). Residual brine materials epsomite ($MgSO_{11}H_{14}$) and hexahydrite ($MgSO_{10}H_{12}$) are also present. Bixbyite (Mn_2O_3), an impurity containing manganese that originated in the $MgCl_2$ brine and was not fully removed through vacuum filtration was also detected. In the 24 wt. % $MgSO_4$+$MgCl_2$ brine flow-through experiments, calcite is the dominant phase observed, and some gypsum was also detected. Residual brine material (epsomite and hexahydrite) alongside the impurity bixbyite and possibly another Mg-Al silicate impurity (Figure 9) were also detected (Figures 9 and 11). Other potential impurity or alteration phases are noted but not identified. No bassanite nor anhydrite is observed in any of the carbonate substrate experiments.

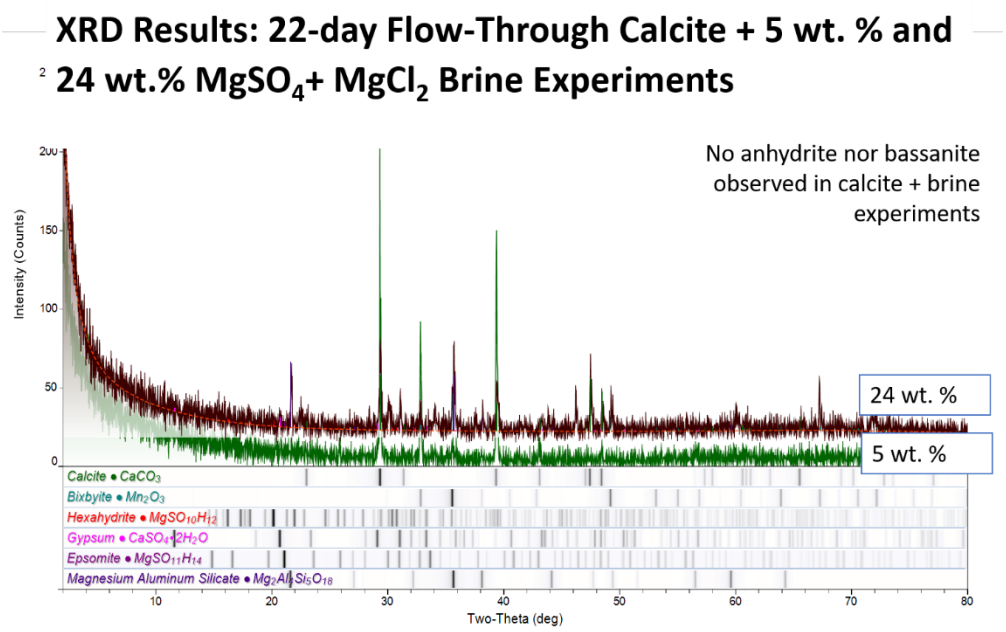

Figure 9. XRD results for 22-day flow-through experimental runs using calcite + 5 wt. % and 24 wt. % brines. Peak positions for calcite, bixbyite, hexahydrite, gypsum, epsomite, and magnesium-aluminum silicate are shown below patterns.

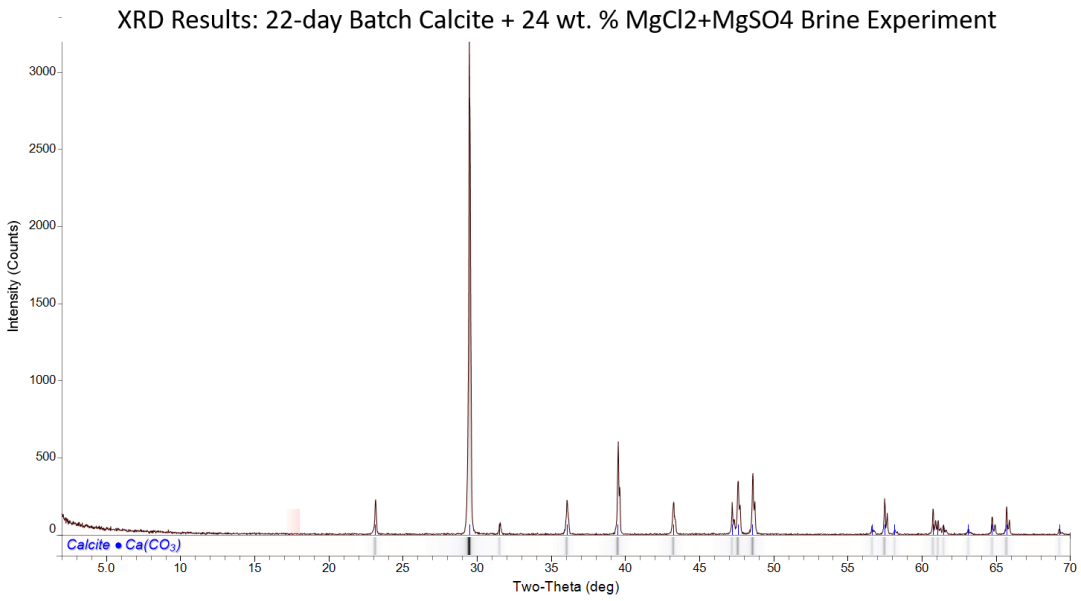

Figure 10. XRD results for 22-day batch experiment using calcite and 24 wt. % brine.

SEM: We analyzed the 24 wt. % $MgSO_4$+$MgCl_2$ brine + calcite flow-through experiment sample via SEM imaging and X-ray mapping. No gypsum was observed, nor was there any significant alteration to calcite grains. Instead, residual brine material was observed as a coating on calcite (Figure 11).

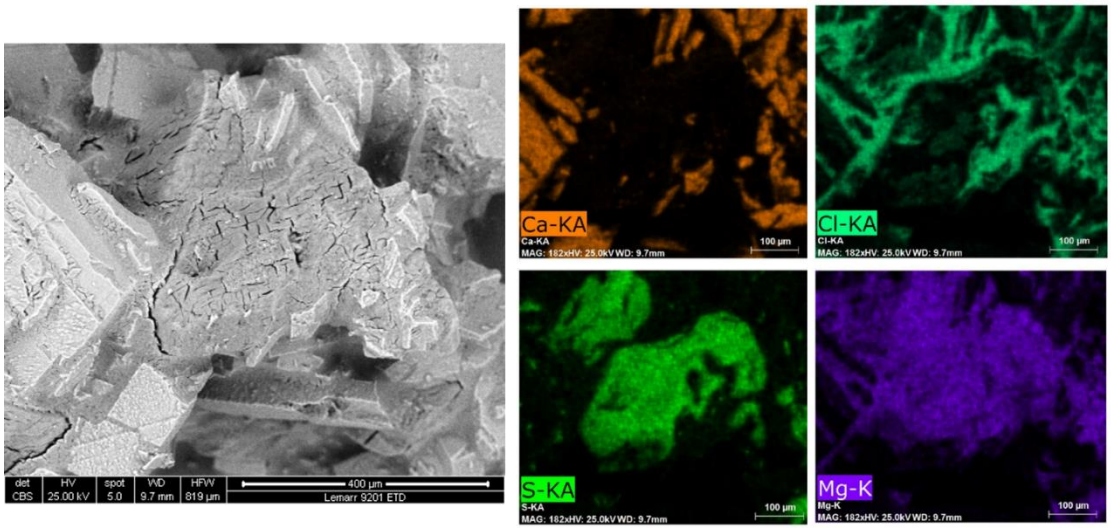

Figure 11. SEM image and EDS maps showing calcite coated with $MgSO_4$ and $MgCl_2$ brine residues.

Discussion

Results Summary

Our jarosite + brine experimental results confirmed that different calcium sulfate minerals form in flow-through experiments compared to batch experiments, despite identical solution chemistries, reaction time, and temperature conditions:

Flow-Through

$$\underbrace{KFe_3(OH)_6(SO_4)_{2\,(s)}}_{\text{Jarosite}} + 3CaCl_{2(aq)} + 5H_2O_{(l)} \rightarrow \underbrace{CaSO_{4(s)}}_{\text{Anhydrite}} + \underbrace{CaSO_4{\cdot}2H_2O_{(s)}}_{\text{Gypsum}} + \underbrace{3FeO(OH,Cl)_{(s)}}_{\text{Akaganeite}} + \underbrace{CaCl_2{\cdot}6H_2O_{(s)}}_{\text{Antarcticite}} + K^+ + Cl^-$$

Batch

$$\underbrace{KFe_3(OH)_6(SO_4)_{2\,(s)}}_{\text{Jarosite}} + 3CaCl_{2(aq)} + 5H_2O_{(l)} \rightarrow \underbrace{2CaSO_4{\cdot}2H_2O_{(s)}}_{\text{Gypsum}} + \underbrace{3FeO(OH,Cl)_{(s)}}_{\text{Akaganeite}} + \underbrace{CaCl_2{\cdot}6H_2O_{(s)}}_{\text{Antarcticite}} + K^+ + Cl^-$$

Over a range of $CaCl_2$ concentrations and water activities, anhydrite is only observed in flow-through experiments, while gypsum is observed in both batch and flow-through experiments. Akaganeite is also formed in abundance in all flow-through and batch experiments. Bassanite may be present in trace amounts in two flow-through experiments but is not observed in batch reactor experiments. Preliminary TEM data (Figure 8) shows calcium enrichment associated with nanoscale minerals on the edges of jarosite in flow-through experiments, though more detailed X-ray maps, point analyses, and transects are needed to fully characterize the nanoscale minerals growing on/attached to the jarosite. Gypsum was the only calcium sulfate phase identified in batch reactor experiments, where it formed relatively large (>1µm) lath-shaped gypsum crystals in the batch experiments (Figures 6a and 7a) that were not observed in flow-

through experiments. These differing mineral assemblages and textures confirm that hydrologic conditions are primary variables affecting calcium sulfate mineralization.

Implications of gypsum formation in jarosite + brine experiments

Gypsum formed in all of our experiments reacting jarosite + $CaCl_2$ brine. Gypsum has also been detected on Mars in several geologic contexts including circumpolar dune fields (Langevin et al., 2005; Masse et al., 2012), at Columbus Crater (Wray et al., 2009), at Meridiani Planum (Clark et al., 2005; Glotch and Bandfield, 2006), at Columbia Hills (Lane et al., 2008), and in mineralized vein sets at Gale Crater (Nachon et al., 2014; Vaniman et al., 2014; Rapin et al., 2016). The gypsum at Gale Crater is of particular interest in our work because it coexists alongside other calcium sulfates – anhydrite and bassanite – with differing hydration states. Our results indicate that gypsum is kinetically preferred in closed-system batch experiments where we observe aggregation of smaller crystallites into relatively large (1-2 micron) crystal laths. These lath-shaped gypsum crystals were not observed in flow-through experiments, though gypsum was detected in these samples via XRD. The lath shaped gypsum identified in batch reactor experiments exhibited significant electron beam sensitivity in the 80kV and 200kV TEMs. Similar beam sensitive behavior was observed around jarosite grains in flow-through experiments on the same instruments. While not a primary line of evidence, this observation spurred our more detailed analyses of reaction products around the edges of jarosite grains in flow-through experiments. The significant morphological differences between calcium sulfate phases in batch and flow-through experiments suggests separate nucleation pathways for

calcium sulfate minerals in differing hydrodynamic conditions similar to those postulated by Bystriansky et al. (2016) where calcium sulfates in jar (batch) experiments are thought to crystallize via "bulk nucleation," but heterogeneous nucleation dominates reverse osmosis (flow-through) experiments.

Implications of anhydrite formation in jarosite + brine experiments

Our experiments found that anhydrite can also form relatively quickly from flowing brines reacted with jarosite, even when the activity of water is near or above the anhydrite stability field, but anhydrite does not form in closed system experiments, confirming observations reported by Dixon et al. (2015). Anhydrite has been detected in association with bassanite and gypsum in sediments at Yellowknife Bay, Gale Crater (Nachon et al., 2014; Vaniman et al., 2014; Rapin et al., 2016). This observation spurred renewed interest in the kinetics and thermodynamics of the calcium sulfate system. Though anhydrite is the most thermodynamically stable calcium sulfate phase in high salinity brines, closed system batch experiments have routinely demonstrated gypsum formation instead (Posnjak, 1940; Hardie, 1967; Freyer and Voigt, 2003; Fu et al., 2012). However, Dixon et al. (2015) showed anhydrite formation in flowing high salinity brine at low temperatures over a relatively brief period (3 weeks) while gypsum was observed in batch experiments under the same conditions. Here, we have demonstrated anhydrite formation across a range of salinities in flowing brines, while gypsum is still the only calcium sulfate to form in batch experiments. In our results, both anhydrite and gypsum were detected in flow-through experiments. The relatively broad width of anhydrite and gypsum peaks observed via XRD in jarosite + brine flow-

through experiments (Figure 2) supports the case for nanoscale calcium sulfate in these flow-through experiments (Monshi et al., 2012).

We suggest that the formation of anhydrite (and perhaps also gypsum) results through heterogeneous nucleation of calcium sulfate phases on jarosite grains analogous to the Bystriansky et al. (2016) finding that calcium sulfates formed via heterogeneous nucleation on the membrane surface in reverse osmosis experiments. Slight calcium enrichments were also observed on jarosite surfaces in TEM (Figure 8). Marked textural differences between the large lath-shaped gypsum particles in batch experiments contrasted with the nanoscale mineral nucleation at the edges of jarosite grains (Figures 6b, 7d, and 8) also suggests a heterogeneous nucleation pathway for calcium sulfate formation in flow-through experiments.

Implications of possible bassanite formation in jarosite + brine experiments

We observed possible bassanite formation in two flow-through experiments. Bassanite, the partially hydrated intermediate calcium sulfate phase, has been proposed to form on Mars via dehydration (Vaniman et al., 2017) in a warmer paleoclimate (Vaniman et al., 2008; Vaniman et al., 2009), through diagenesis of gypsum after burial, or potentially through hydrothermal activity (Vaniman et al., 2008). Rapin et al. (2016) suggested that bassanite also may form through partial hydration of anhydrite in aqueous solution. In lab settings, bassanite was observed to form as a metastable precursor phase to gypsum formation (Van Driessche et al., 2012). However, since bassanite is a somewhat dubious or trace phase in our experiments, we are not able to say anything definitively about bassanite formation.

Implications of akaganeite formation in jarosite + brine experiments

Jarosite + $CaCl_2$ brines readily formed akaganeite in all of our experiments. On Mars, akaganeite has been detected from orbit in several locations (Carter et al., 2015) and by the MSL rover at Yellowknife Bay, Gale Crater (Ming et al., 2014; Grotzinger et al., 2014; Vaniman et al., 2014). Akaganeite occurs on Earth in association with jarosite and acid sulfate systems in chloride rich environments (Johnson, 1977; Bibi et al., 2011) and as a corrosion product of metallic iron-bearing solid phases and solutions in Cl-rich environments under acidic oxidizing conditions (Peretyazhko et al., 2016). In lunar rocks, akaganeite has been identified as a probable alteration product in Apollo 16 samples, but is considered by Taylor et al. (1974) and Haggerty (1978) to have formed because of contamination by terrestrial water vapor of $FeCl_2$-bearing lunar rocks. However, more recent experimental work by Shearer et al. (2014) argues that the akaganeite in question may have a lunar origin after all. Similar terrestrial contamination questions also plague the interpretation of akaganeite in meteorites (Bland et al., 1997).

Some workers (Carter et al., 2015) have postulated that the presence of akaganeite on Mars may be indicative of past or ongoing biologic activity on Mars. However, while biogenic formation of akaganeite has been recorded on Earth (Chan et al., 2004; Fortin and Langley, 2005; Xiong et al., 2008; Brayner et al., 2009), our results along with those of others (Ohtsuka, 1996; Weckler and Lutz, 1998; Rémazeilles and Refait, 2007) show that akaganeite readily forms inorganically in a range of salinities and hydrodynamic conditions when chloride salts are present and, therefore, is not indicative of biologic activity. In addition to providing further evidence for inorganic

formation of akaganeite, a somewhat surprising component of our results was the large amount (up to ~40 wt. %) of akageneite observed across jarosite + brine experiments. Pritchett et al. (2012) and Elwood Madden et al. (2012) also reported iron oxides forming in jarosite dissolution experiments. In flow-through experiments, calcium sulfate phases may be associated with akaganeite, both of which seem to be growing as nanoscale minerals around the edges of microscale jarosite grains (Figures 6a, 7d, and 8); more X-ray mapping is needed to confirm this. Akaganeite was also observed separate from jarosite grains as seen in Figure 6e in addition to on the surface (Figures 7c,d,f and 8), suggesting akageneite forms via both homogeneous nucleation within the brine and as heterogeneous growth on the surface of pre-existing jarosite.

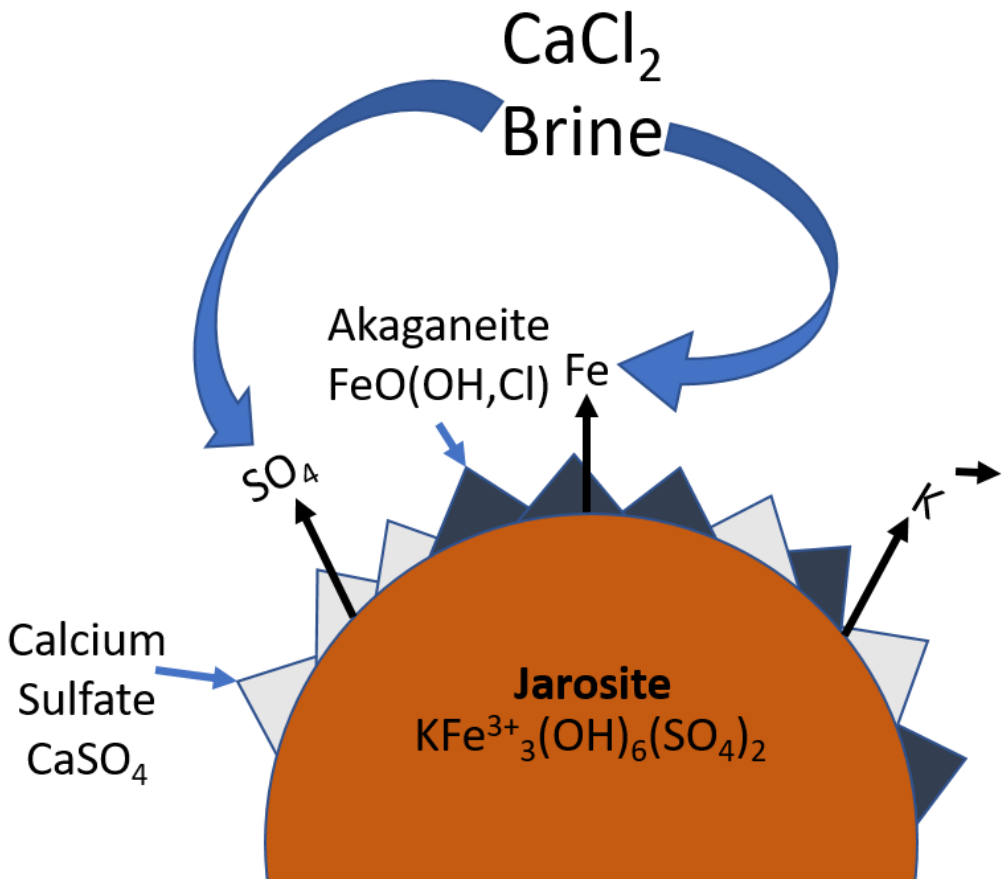

Figure 12. Model of suggested heterogeneous calcium sulfate and akageneite nucleation and growth and jarosite in flow-through experiments.

Carbonate experiment results

In the calcite + brine experiments, gypsum is observed as a reaction product in the 24 wt. % $MgSO_4$ + $MgCl_2$ flow-through experiment; no other calcium sulfates were formed in other experimental runs including batch reactor experiments. The absence of anhydrite in these flow-through samples supports our hypothesis that anhydrite formation in jarosite + brine flow-through experiments is controlled by mineral substrate or by the presence of other ions (iron or potassium) in solution in addition to hydrodynamic conditions. Though not a directly analogous study because it was performed at higher temperature (95℃), Guan et al. (2009) reported that high potassium ion concentration (>0.173M) resulted in anhydrite formation through gypsum dehydration and posited that this could be due to potassium inhibiting bassanite nucleation and growth. Recent work by Bystriansky et al. (2016) indicated that, when iron ions are present in solution in batch and flow-through reverse osmosis experiments, calcium sulfate scale crystallizes more quickly. In this work, reverse osmosis experiments yielded faster calcium sulfate crystallization than batch tests, and Bystriansky et al. (2016) attributes this difference to heterogeneous nucleation on the membrane surface in reverse osmosis experiments and bulk crystallization in the batch experiments.

Implications for Mars

Jarosite and abundant salts have been extensively documented on the martian surface by both orbiters and rovers (King and McLennan, 2010; Wray et al., 2010; Squyers et al., 2012; Hausrath and Brantley, 2010; Arvidson et al., 2006; Vaniman et al.,

2014; Nachon et al., 2014; Ojha et al., 2014; Toner et al., 2015). Anhydrite has been observed in association with jarosite at Gale Crater (Vaniman et al., 2014; Nachon et al., 2014). In the Sheepbed Mudstone, the mineralogical assemblage jarosite, anhydrite, bassanite, and akageneite is observed, which suggests that this formation may have experienced flowing chloride brines in a near-surface diagenetic environment (Rampe et al., 2015). Therefore, the mineralogical assemblages observed in our experiments can be applied to the study of the diagenetic histories of martian rocks.

The presence of anhydrite in flow-through experiments with relatively high activities (a_w = 0.98 - 0.8) of water negates Dixon's hypothesis that anhydrite nucleates due to sustained low water activity in high salinity, flowing brine. Instead, anhydrite was observed forming in all three brine concentrations after 22 days of reaction, despite significantly higher water activities in the 20 and 5 wt.% brines. Again, no anhydrite was observed in any of the batch reactor experiments, suggesting hydrodynamic effects are key for anhydrite formation and growth at low temperatures in the presence of jarosite.

Previous studies have interpreted anhydrite veins on Mars as forming at depth from pre-existing gypsum indicating significant burial had occurred prior to diagenesis (Vaniman et al., 2014; Bristow et al., 2015). However, our experimental results demonstrate that anhydrite can also form initially from jarosite alteration in $CaCl_2$ brines without a pre-existing gypsum phase at lower temperatures if there is groundwater flow. Akaganeite is also observed in these deposits, suggesting that chloride-rich brines could have been active in these rocks. Linking calcium sulfate phase nucleation to specific hydrodynamic conditions gives us information about the open or closed nature of the aqueous system in which the observed calcium sulfate minerals may have formed.

Ultimately, our findings can provide much needed data for interpreting the timing and evolution of depositional environments and diagenetic conditions for the sedimentary rocks at Gale Crater and other locations where calcium sulfate minerals have been observed (Grotzinger et al., 2015; Stack et al., 2016; Borlina et al., 2015; Anderson et al., 2015; Grant et al., 2014).

Conclusions

Our results suggest that anhydrite can readily form at low temperatures from calcium-rich brines reacting with sulfate released from jarosite, calling into question previous interpretations that assumed anhydrite only forms at moderate-high temperatures or over long periods of high salinity diagenesis. This is particularly relevant to anhydrite detected on Mars because it presents an alternative means of forming anhydrite that does not require elevated temperatures due to burial and gypsum dehydration. We posit that, given certain mineralogical substrates, anhydrite could form near the martian surface in flowing high salinity groundwater conditions. Our argument is further supported by the abundant akaganeite observed in our experiments and on Mars in association with both calcium sulfates and jarosite.

References

Anderson, R., Bridges, J. C., Williams, A., Edgar, L., Ollila, A., Williams, J., ... & Gupta, S. (2015). ChemCam results from the Shaler outcrop in Gale crater, Mars. *Icarus*, *249*, 2-21.

Arvidson, R. E., et al. (2006), Nature and origin of the hematite-bearing plains of Terra Meridiani based on analyses of orbital and Mars Exploration rover data sets, *Journal of Geophysical Research-Planets*, *111*(E12).

Aubrey, A., Cleaves, H. J., Chalmers, J. H., Skelley, A. M., Mathias, R. A., Grunthaner, F. J., Ehrenfreund, P., and Bada, J. L. (2006) Sulfate minerals and organic compounds on Mars. *Geology 3*4(5), 357–360.

Bibi, I., Singh, B., & Silvester, E. (2011). Akaganéite (β-FeOOH) precipitation in inland acid sulfate soils of south-western New South Wales (NSW), Australia. *Geochimica et Cosmochimica Acta*, *75*(21), 6429-6438.

Bibring, J. P., Langevin, Y., Mustard, J. F., Poulet, F., Arvidson, R., Gendrin, A., ... & Berthé, M. (2006). Global mineralogical and aqueous Mars history derived from OMEGA/Mars Express data. *Science*, *312*(5772), 400-404.

Bishop, J. L. (2016) Personal communication.

Bland, P. A., Kelley, S. P., Berry, F. J., Cadogan, J. M., & Pillinger, C. T. (1997). Artificial weathering of the ordinary chondrite Allegan: Implications for the presence of Cl–as a structural component in akaganeite. *American Mineralogist*, *82*(11-12), 1187-1197.

Borlina C. S., Ehlmann B. L., and Kite E. S. (2015) Modeling the thermal and physical evolution of Mount Sharp's sedimentary rocks, Gale crater, Mars: Implications for diagenetic minerals on the MSL Curiosity Rover traverse. J Geophys Res 120(8):1396–1414.

Brass, G. W. (1980) Stability of Brines on Mars. *Icarus* 42, 20-28.

Brayner, R., Yéprémian, C., Djediat, C., Coradin, T., Herbst, F., Livage, J., ... & Couté, A. (2009). Photosynthetic microorganism-mediated synthesis of akaganeite (β-FeOOH) nanorods. *Langmuir*, *25*(17), 10062-10067.

Bridges, J. C., Catling, D. C., Saxton, J. M., Swindle, T. D., Lyon, I. C., & Grady, M. M. (2001). Alteration assemblages in Martian meteorites: Implications for near-surface processes. In *Chronology and evolution of Mars* (pp. 365-392). Springer Netherlands.

Bristow T. F. et al. (2015) The origin and implications of clay minerals from Yellowknife Bay, Gale crater, Mars. Am Mineral 100(4):824–836.

Bristow, T. F., Haberle, R. M., Blake, D. F., Des Marais, D. J., Eigenbrode, J. L., Fairén, A. G., ... & Siebach, K. L. (2016). Low Hesperian PCO2 constrained from in situ mineralogical analysis at Gale Crater, Mars. *Proceedings of the National Academy of Sciences*, *114*(9), 2166-2170.

Bystriansky, M., Nir, O., Sir, M., Honzajkova, Z., Vurm, R., Hrychova, P., Bervic, A. and van der Bruggen, B. (2016) The presence of ferric iron promotes calcium sulphate scaling in reverse osmosis processes. *Desalination 393*, 115-119.

Carter, J., Viviano-Beck, C., Loizeau, D., Bishop, J., & Le Deit, L. (2015). Orbital detection and implications of akaganeite on Mars. *Icarus*, *253*, 296-310.

Clark, B. C. (1978) Implications of abundant hydroscopic salts in the martian regolith. *Icarus* 34, 645-665.

Clark, B. C. (1993). Geochemical components in Martian soil. *Geochimica et Cosmochimica acta*, *57*(19), 4575-4581.

Clark, B. C., Morris, R. V., McLennan, S. M., Gellert, R., Jolliff, B., Knoll, A. H., ... & Yen, A. (2005). Chemistry and mineralogy of outcrops at Meridiani Planum. *Earth and Planetary Science Letters*, *240*(1), 73-94.

Chan, C. S., De Stasio, G., Welch, S. A., Girasole, M., Frazer, B. H., Nesterova, M. V., ... & Banfield, J. F. (2004). Microbial polysaccharides template assembly of nanocrystal fibers. *Science*, *303*(5664), 1656-1658.

Christensen, P. R., M. B. Wyatt, T. D. Glotch , A. D. Rogers, S. Anwar, R. E. Arvidson, J. L. Bandfield, D. L. Blaney, C. Budney, W. M. Calvin, A. Faracaro, R. L. Fergason, N. Gorelick, T. G. Graff, V. E. Hamilton, A. G. Hayes, J. R. Johnson, A. T. Knudson, H. Y. McSween, G. L. Mehall, L. K. Mehall, J. E. Moersch, R. V. Morris, M. D. Smith, S. W. Squyres, S. W. Ruff, and M. J. Wolff (2004), Mineralogy at Meridiani Planum from the Mini-TES experiment on the Opportunity Rover, *Science*, *306*, 1733-1739.Clark, B. C. (1993), Geochemical components in Martian soil, *Geochimica et Cosmochimica Acta*, *57*, 4575-4581.Clark, B. C., R. V. Morris, S. M. McLennan, R. Gellert, B. Jolliff, A. H. Knoll, S. W. Squyres, T. K. Lowenstein, D. W. Ming, N. J. Tosca, A. Yen, P. R. Christensen, S. Gorevan, J. Bruckner, W. Calvin, G. Dreibus, W. Farrand, G. Klingelhoefer, H. Waenke, J. Zipfel, J. F. Bell, J. Grotzinger, H. Y. McSween, and R. Rieder (2005), Chemistry and mineralogy of outcrops at Meridiani Planum, *Earth and Planetary Science Letters*, *240*, 73-94.

Dixon, E. M., Elwood Madden, A. S., Hausrath, E. M., & Elwood Madden, M. E. (2015). Assessing hydrodynamic effects on jarosite dissolution rates, reaction

products, and preservation on Mars. *Journal of Geophysical Research: Planets*, *120*(4), 625-642.

Driscoll R. and Leinze R. (2005) In Methods for Synthesis of Some Jarosites: U.S. Geological Survey Techniques and Methods, 05–D1 (ed. U. S. G. Survey). pp. 6.D1 (ed. U. S. G. Survey). pp. 6.

Elsenousy, A, Hanley, J, and Chevrier, V. F. (2015) Effect of evaporation and freezing on the salt paragenesis and habitability of brines at the Phoenix landing site. *Earth and Planetary Science Letters* 421, 39-46.

Elwood Madden, M. E., Bodnar, R. J., & Rimstidt, J. D. (2004). Jarosite as an indicator of water-limited chemical weathering on Mars. *Nature*, *431*(7010), 821-823.

Elwood Madden, M. E., Madden, A. S., Rimstidt, J. D., Zahrai, S., Kendall, M. R., & Miller, M. A. (2012). Jarosite dissolution rates and nanoscale mineralogy. *Geochimica et Cosmochimica Acta*, *91*, 306-321.

Fortin, D., & Langley, S. (2005). Formation and occurrence of biogenic iron-rich minerals. *Earth-Science Reviews*, *72*(1), 1-19.

Freyer, D., & Voigt, W. (2003). Crystallization and phase stability of CaSO 4 and CaSO 4–based salts. *Monatshefte für Chemie/Chemical Monthly*, *134*(5), 693-719.

Fu, C., Zhou, Y., Liu, G., Huang, J., Wu, W., & Sun, W. (2012). Carboxylate-ended poly (ethylene glycol) macromonomers and their copolymers as inhibitors for calcium phosphate and calcium sulfate. *International Journal of Polymeric Materials*, *61*(5), 341-356.

Gendrin, A., Mangold, N., Bibring, J. P., Langevin, Y., Gondet, B., Poulet, F., ... & LeMouélic, S. (2005). Sulfates in Martian layered terrains: the OMEGA/Mars Express view. *Science*, *307*(5715), 1587-1591.

Glotch, T. D., and P. R. Christensen (2005), Geologic and mineralogic mapping of Aram Chaos: Evidence for a water-rich history, *Journal of Geophysical Research-Planets, 110*.

Glotch, T. D., & Bandfield, J. L. (2006). Determination and interpretation of surface and atmospheric Miniature Thermal Emission Spectrometer spectral end-members at the Meridiani Planum landing site. Journal of Geophysical Research: Planets, 111(E12).

Glotch, T. D., & Rogers, A. D. (2007). Evidence for aqueous deposition of hematite-and sulfate-rich light-toned layered deposits in Aureum and Iani Chaos, Mars. *Journal of Geophysical Research: Planets*, *112*(E6).

Gooding, J. L., Wentworth, S. J., & Zolensky, M. E. (1988). Calcium carbonate and sulfate of possible extraterrestrial origin in the EETA 79001 meteorite. *Geochimica et Cosmochimica Acta*, *52*(4), 909-915.

Gooding, J. L., Wentworth, S. J., & Zolensky, M. E. (1991). Aqueous alteration of the Nakhla meteorite. *Meteoritics & Planetary Science*, *26*(2), 135-143.

Grant, J. A., Wilson, S. A., Mangold, N., Calef, F., & Grotzinger, J. P. (2014). The timing of alluvial activity in Gale crater, Mars. *Geophysical Research Letters*, *41*(4), 1142-1149.

Grotzinger JP, et al.; MSL Science Team (2014) A habitable fluvio-lacustrine environment at Yellowknife Bay, Gale crater, Mars. Science 343(6169):1242777.

Grotzinger, J. P., Gupta, S., Malin, M. C., Rubin, D. M., Schieber, J., Siebach, K., ... & Calef, F. (2015). Deposition, exhumation, and paleoclimate of an ancient lake deposit, Gale crater, Mars. *Science*, *350*(6257), aac7575.

Guan, B., Yang, L., Wu, Z., Shen, Z., and Ye, Q. (2009) Preparation of Alpha-calcuim sulfate hemihydrate from FGD gypsum in K, Mg-containing concentrated CaCl2 solution under mild conditions. Fuel 88, 1286-1293.

Haggerty, S. E. (1978). Apollo 16 deep drill-A review of the morphological characteristics of oxyhydrates on rusty particle 60002, 108, determined by SEM. In *Lunar and Planetary Science Conference Proceedings* 9, 1861-1874.

Hardie, L. A. (1967), The gypsum-anhydrite equilibrium at one atmospheric pressure, *American Mineralogist*, *52*, 171-200.

Hausrath, E. M., and S. L. Brantley (2010), Basalt and olivine dissolution under cold, salty, and acidic conditions: What can we learn about recent aqueous weathering on Mars? *Journal of Geophysical Research-Planets*, *115.*

He, S., Oddo, J. E., and Tomson, M. B. (1994) The nucleation kinetics of calcium sulfate dehydrate in NaCl solutions up to 6m and 90°C. Journal of Colloid and Interface Science 162, 297-303.

Hecht, M. H., S. P. Kounaves, R. C. Quinn, S. J. West, S. M. M. Young, D. W. Ming, D. C. Catling, B. C. Clark, W. V. Boynton, J. Hoffman, L. P. DeFlores, K. Gospodinova, J. Kapit, and P. H. Smith (2009), Detection of Perchlorate and the Soluble Chemistry of Martian Soil at the Phoenix Lander Site, *Science*, *325*, 64-67.

Hurowitz, J. A., and W. W. Fischer (2014), Contrasting styles of water–rock interaction at the Mars Exploration Rover landing sites, *Geochimica et Cosmochimica Acta*, *127*, 25-38.

Hurowitz, J.A. and McLennan, S.M. (2007) A similar to 3.5 Ga record of water-limited, acidic weathering conditions on Mars. Earth and Planetary Science Letters 260, 432-443.

Hu, G., Dam-Johansen, K., and Wedel, S. (2007) Oriented Nucleation and Growth of Anhydrite during Direct Sulfation of Limestone. Crystal Growth and Design, 8, 1181-1185.

Johnston, J. H. (1977) Jarosite and akaganéite from White Island volcano, New Zealand: an X-ray and Mössbauer study. *Geochimica et Cosmochimica Acta* 41.4: 539-544.

King, P. L., and S. M. McLennan (2010), Sulfur on Mars, *Elements*, *6*(2), 107-112.

Klingelhöfer, G., R. V. Morris, B. Bernhardt, C. Schroder, D. S. Rodionov, P. A. de Souza, A. Yen, R. Gellert, E. N. Evlanov, B. Zubkov, J. Foh, E. Kankeleit, P. Gutlich, D. W. Ming, F. Renz, T. Wdowiak, S. W. Squyres, and R. E. Arvidson (2004), Jarosite and hematite at Meridiani Planum from Opportunity's Mossbauer spectrometer, *Science*, *306*, 1740-1745.

Lafuente B, Downs R T, Yang H, Stone N (2015) The power of databases: the RRUFF project. In: Highlights in Mineralogical Crystallography, T Armbruster and R M Danisi, eds. Berlin, Germany, W. De Gruyter, pp 1-30.

Lane, M. D., Bishop, J. L., Dyar, M. D., King, P. L., Parente, M., & Hyde, B. C. (2008). Mineralogy of the Paso Robles soils on Mars. *American Mineralogist*, *93*(5-6), 728-739.

Langevin, Y., Poulet, F., Bibring, J. and Gondet, B. (2005) Sulfates in the North Polar Region of Mars detected by OMEGA/Mars Express. *Science* 307, 1584-1586.

Mangold, N., Gendrin, A., Gondet, B., LeMouelic, S., Quantin, C., Ansan, V., ... & Neukum, G. (2008). Spectral and geological study of the sulfate-rich region of West Candor Chasma, Mars. *Icarus*, *194*(2), 519-543.

Masse, M., O. Bourgeois, S. Le Mouelic, C. Verpoorter, A. Spiga, and L. Le Deit (2012), Wide distribution and glacial origin of polar gypsum on Mars, *Earth and Planetary Science Letters*, *317*, 44-55.

McCubbin, F. M., Tosca, N. J., Smirnov, A., Nekvasil, H., Steele, A., Fries, M., & Lindsley, D. H. (2009). Hydrothermal jarosite and hematite in a pyroxene-hosted melt inclusion in martian meteorite Miller Range (MIL) 03346: Implications for magmatic-hydrothermal fluids on Mars. *Geochimica et Cosmochimica Acta*, *73*(16), 4907-4917.

McLennan, S. M., J. F. Bell, W. M. Calvin, P. R. Christensen, B. C. Clark, P. A. de Souza, J. Farmer, W. H. Farrand, D. A. Fike, R. Gellert, A. Ghosh, T. D. Glotch, J. P. Grotzinger, B. Hahn, K. E. Herkenhoff, J. A. Hurowitz, J. R. Johnson, S. S. Johnson, B. Jolliff, G. Klingelhofer, A. H. Knoll, Z. Learner, M. C. Malin, H. Y. McSween, J. Pocock, S. W. Ruff, L. A. Soderblom, S. W. Squyres, N. J. Tosca, W. A. Watters, M. B. Wyatt, and A. Yen (2005), Provenance and diagenesis of the evaporite-bearing Burns formation, Meridiani Planum, Mars. *Earth and Planetary Science Letters, 240*, 95-121.

Ming, D. W., Archer, P. D., Glavin, D. P., Eigenbrode, J. L., Franz, H. B., Sutter, B., ... & Mahaffy, P. R. (2014). Volatile and organic compositions of sedimentary rocks in Yellowknife Bay, Gale Crater, Mars. *Science*, *343*(6169), 1245267.

Monshi, A., Foroughi, M. R., and Monshi, M. R. (2012) Modified Scherrer Equation to estimate more accurately nano-crystallite size using XRD. *World Journal of Nano Science and Engineering*, Vol. 2 No. 3, 2012, pp. 154-160.

Mullin, J. W. (1993) Crystallization, 3rd Butterworth-Heinemann, Oxford.

Murchie, S. L., J. F. Mustard, B. L. Ehlmann, R. E. Milliken, J. L. Bishop, N. K. McKeown, E. Z. N. Dobrea, F. P. Seelos, D. L. Buczkowski, S. M. Wiseman, R. E. Arvidson, J. J. Wray, G. Swayze, R. N. Clark, D. J. D. Marais, A. S. McEwen, and J. P. Bibring (2009), A synthesis of Martian aqueous mineralogy after 1 Mars year of observations from the Mars Reconnaissance Orbiter, *Journal of Geophysical Research – Planets, 114*.

Nachon, M., Clegg, S.M., Mangold, N., Schroeder, S., Kah, L.C., Dromart, G., Ollila, A., Johnson, J.R., Oehler, D.Z., Bridges, J.C., Le Mouelic, S., Forni, O., Wiens, R.C., Anderson, R.B., Blaney, D.L., Bell, J.F., Clark, B., Cousin, A., Dyar, M.D., Ehlmann, B., Fabre, C., Gasnault, O., Grotzinger, J., Lasue, J., Lewin, E., Leveille, R., McLennan, S., Maurice, S., Meslin, P.Y., Rapin, W., Rice, M., Squyres, S.W., Stack, K., Sumner, D.Y., Vaniman, D. and Wellington, D. (2014) Calcium sulfate veins characterized by ChemCam/Curiosity at Gale crater, Mars. Journal of Geophysical Research-Planets 119, 1991-2016.

Ohtsuka, T. (1996) Raman spectra of passive films of iron in neutral borate solution. *Materials Transactions* 37, 67-69.

Ojha, L., Wilhelm, M. B., Murchie, S. L., McEwen, A. S., Wray, J. J., Hanley, J., ... & Chojnacki, M. (2015). Spectral evidence for hydrated salts in recurring slope lineae on Mars. *Nature Geoscience*, *8*(11), 829-832.

Ossorio, M., A.E.S. Van Driessche, P. Perez, and J.M. Garcia-Ruiz (2014), The gypsum-anhydrite paradox revisited, *Chemical Geology*, 386, 16-21.

Osterloo, M. M., V. E. Hamilton, J. L. Bandfield, T. D. Glotch, A. M. Baldridge, P. R. Christensen, L. L. Tornabene, and F. S. Anderson (2008), Chloride-bearing materials in the southern highlands of Mars, *Science, 319*, 1651-1654.

Peretyazhko, T. S., Fox, A., Sutter, B., Niles, P. B., Adams, M., Morris, R. V., & Ming, D. W. (2016). Synthesis of akaganeite in the presence of sulfate: Implications for akaganeite formation in Yellowknife Bay, Gale Crater, Mars. *Geochimica et Cosmochimica Acta*, *188*, 284-296.

Pritchett, B. N., Madden, M. E., & Madden, A. S. (2012). Jarosite dissolution rates and maximum lifetimes in high salinity brines: Implications for Earth and Mars. *Earth and Planetary Science Letters*, *357*, 327-336.

Pina, C.M. (2009) Nanoscale dissolution and growth on anhydrite cleavage faces. *Geochimica et Cosmochimica Acta 73*, 7034-7044.

Posnjak, E. (1940), Deposition of calcium sulfate from sea water, *American Journal of Science*, *238*(8), 559-568.

Rampe, E. B., Morris, R. V., Bish, D. L., Chipera, S. J., Ming, D. W., Blake, D. F., ... & Morrison, S. M. (2015). Potential cement phases in sedimentary rocks drilled by Curiosity at Gale Crater, Mars. *LPSC Abs*. 2038.

Rao, M. N., L. E. Nyquist, S. R. Sutton, G. Dreibus, D. H. Garrison, and J. Herrin (2009), Fluid-evaporation records preserved in salt assemblages in Meridiani rocks, *Earth and Planetary Science Letters*, *286*(3-4), 396-403.

Rapin, W., Meslin, P.Y., Maurice, S., Vaniman, D., Nachon, M., Mangold, N., Schroder, S., Gasnault, O., Forni, O., Wiens, R.C., Martinez, G.M., Cousin, A., Sautter, V., Lasue, J., Rampe, E.B. and Archer, D. (2016) Hydration state of calcium sulfates in Gale crater, Mars: Identification of bassanite veins. Earth and Planetary Science Letters 452, 197-205.

Rémazeilles, C., & Refait, P. (2007). On the formation of β-FeOOH (akaganéite) in chloride-containing environments. *Corrosion Science*, *49*(2), 844-857.

Rieder, R., R. Gellert, R. C. Anderson, J. Bruckner, B. C. Clark, G. Dreibus, T. Economou, G. Klingelhoffer, G. W. Lugmair, D. W. Ming, S. W. Squyres, C. d'Uston, H. Wanke, A. Yen, and J. Zipfel (2004), Chemistry of rocks and soils at Meridiani Planum from the alpha particle X-ray spectrometer, *Science*, *306*, 1746-1749.

Shearer, C. K., Sharp, Z. D., Burger, P. V., McCubbin, F. M., Provencio, P. P., Brearley, A. J., & Steele, A. (2014). Chlorine distribution and its isotopic composition in “rusty rock” 66095. Implications for volatile element enrichments of

"rusty rock" and lunar soils, origin of "rusty" alteration, and volatile element behavior on the Moon. *Geochimica et Cosmochimica Acta*, *139*, 411-433.

Sohnel, O. and Garside, J. (1992) Precipitation: basic principles and industrial applications, Butterworth-Heinemann.

Stack, K. M., Edwards, C. S., Grotzinger, J. P., Gupta, S., Sumner, D. Y., Calef, F. J., ... & Le Deit, L. (2016). Comparing orbiter and rover image-based mapping of an ancient sedimentary environment, Aeolis Palus, Gale crater, Mars. *Icarus*, *280*, 3-21.

Stawski, T. M., Van Driessche, A. E., Ossorio, M., Rodriguez-Blanco, J. D., Besselink, R., & Benning, L. G. (2016). Formation of calcium sulfate through the aggregation of sub-3 [thinsp] nanometre primary species. *Nature communications*, *7*.

Squyres, S. W., J. P. Grotzinger, R. E. Arvidson, J. F. Bell, W. Calvin, P. R. Christensen, B. C. Clark, J. A. Crisp, W. H. Farrand, K. E. Herkenhoff, J. R. Johnson, G. Klingelhofer, A. H. Knoll, S. M. McLennan, H. Y. McSween, R. V. Morris, J. W. Rice, R. Rieder, and L. A. Soderblom (2004), In situ evidence for an ancient aqueous environment at Meridiani Planum, Mars, *Science, 306*, 1709-1714.

Squyres, S. W., Arvidson, R. E., Bell, J. F., Calef, F., Clark, B. C., Cohen, B. A., ... & Grant, J. (2012). Ancient impact and aqueous processes at Endeavour Crater, Mars. *Science*, *336*(6081), 570-576.

Taylor, L. A., Mao, H. K., & Bell, P. M. (1974). beta-FeOOH, akaganeite, in lunar rocks. In *Lunar and Planetary Science Conference Proceedings* (Vol. 5, pp. 743-748).

Toner, J. D., D. C. Catling, B. Light (2014), Soluble salts at the Phoenix Lander site, Mars: A reanalysis of the Wet Chemistry Laboratory data, *Geochimica et Cosmochimica Acta*, *136*, 142-168.

Toner, J. D., Catling, D. C., & Light, B. (2015). Modeling salt precipitation from brines on Mars: Evaporation versus freezing origin for soil salts. *Icarus*, *250*, 451-461.

Tosca, N. J., Knoll, A. H., & McLennan, S. M. (2008). Water activity and the challenge for life on early Mars. *Science*, *320*(5880), 1204-1207.

Van Driessche, A. E. S., L. G. Benning, J. D. Rodriguez-Blanco, M. Ossorio, P. Bots, and J. M. Garcia-Ruiz (2012), The Role and Implications of Bassanite as a Stable Precursor Phase to Gypsum Precipitation, *Science*, *336*(6077), 69-72.

Vaniman, D. T., Bish, D. L., Steve J. Chipera, Claire I. Fialips, J. William Carey, and William C. Feldman. "Magnesium sulphate salts and the history of water on Mars." *Nature* 431, no. 7009 (2004): 663-665.

Vaniman, D. T., Bish, D. L., & Chipera, S. J. (2008, March). Calcium sulfate hydration, stability and transformation on Mars. In *Lunar and Planetary Science Conference* (Vol. 39, p. 1816).

Vaniman, D. T., Bish, D. L., & Chipera, S. J. (2009, March). Bassanite on Mars. In *Lunar and Planetary Science Conference* (Vol. 40, p. 1654).

Vaniman, D. T., Martinez, G. M., Rampe, E. B., Bristow, T. F., Blake, D. F., Yen, A. H., Ming, D. W., Rapin, W., Meslin, P. Y., Grotzinger, J. P., Hazen, R. M., and Crisp, J. A. (2017, March). Calcium sulfates at Gale Crater and limitations of gypsum stability. In *Lunar and Planetary Science Conference* (Vol. 48, p. 1661).

Vaniman, D. T., Bish, D. L., Ming, D. W., Bristow, T. F., Morris, R. V., Blake, D. F., ... & Rice, M. (2014). Mineralogy of a mudstone at Yellowknife Bay, Gale crater, Mars. *Science*, *343*(6169), 1243480.

Wang, A., et al. (2006), Sulfate deposition in subsurface regolith in Gusev crater, Mars, *Journal of Geophysical Research-Planets*, *111*(E2), doi:E02s1710.1029/2005je002513.

Wang, Y. W., Kim, Y. Y., Christenson, H. K., & Meldrum, F. C. (2012). A new precipitation pathway for calcium sulfate dihydrate (gypsum) via amorphous and hemihydrate intermediates. *Chemical Communications*, *48*(4), 504-506.

Warren, JK (1989) Evaporite Sedimentology. Prentice-Hall, Englewood Cliffs, NJ.

Weckler, B. and Lutz, H. D. (1998) Lattice vibration spectra. Part XCV. Infrared spectroscopic studies on the iron oxide hydroxides goethite (α), akaganéite (β), lepidocrocite (γ), and feroxyhite (δ). *European Journal of Solid State and Inorganic Chemistry* 35, 531-544.

Weitz, C.M. and Bishop, J.L. (2016) Stratigraphy and formation of clays, sulfates, and hydrated silica within a depression in Coprates Catena, Mars. *Journal of Geophysical Research-Planets* 121, 805-835.

Wray, J. J., Squyres, S. W., Roach, L. H., Bishop, J. L., Mustard, J. F., & Dobrea, E. Z. N. (2010). Identification of the Ca-sulfate bassanite in Mawrth Vallis, Mars. *Icarus*, *209*(2), 416-421.

Wray, J. J., R. E. Milliken, C. M. Dundas, G. A. Swayze, J. C. Andrews-Hanna, A. M. Baldridge, M. Chojnacki, J. L. Bishop, B. L. Ehlmann, S. L. Murchie, R. N. Clark, F. P. Seelos, L. L. Tornabene, and S. W. Squyres (2011), Columbus crater and other possible groundwater-fed paleolakes of Terra Sirenum, Mars, *Journal of Geophysical Research*, 116 (E01001).

Taylor, L. A., Mao, H. K., & Bell, P. M. (1974). Identification of the hydrated iron oxide mineral akaganéite in Apollo 16 lunar rocks. *Geology*, *2*(9), 429-432.

Xiong, H., Liao, Y., Zhou, L., Xu, Y., & Wang, S. (2008). Biosynthesis of nanocrystal akaganeite from FeCl2 solution oxidized by Acidithiobacillus ferrooxidans cells. *Environmental science & technology*, *42*(11), 4165-4169.

Yen, A. S., R. Gellert, C. Schroder, R. V. Morris, J. F. Bell, A. T. Knudson, B. C. Clark, D. W. Ming, J. A. Crisp, R. E. Arvidson, D. Blaney, J. Bruckner, P. R. Christensen, D. J. DesMarais, P. A. de Souza, T. E. Economou, A. Ghosh, B. C. Hahn, K. E. Herkenhoff, L. A. Haskin, J. A. Hurowitz, B. L. Joliff, J. R. Johnson, G. Klingelhofer, M. B. Madsen, S. M. McLennan, H. Y. McSween, L. Richter, R. Rieder, D. Rodionov, L. Soderblom, S. W. Squyres, N. J. Tosca, A. Wang, M. Wyatt, and J. Zipfel (2005), An integrated view of the chemistry and mineralogy of martian soils, *Nature, 436*, 49-54.

Zen, E. A. (1965), Solubility measurements in the system $CaSO_4$-NaCl-H_20 at 35°, 50°, and 70° C and one atmosphere pressure, *Journal of Petrology*, *6*, 124-164.